# Influence of POSS nano-particles on Sn–3.0Ag–0.5Cu–xPOSS/Cu composite solder joints during isothermal aging

**Jun Shen · Qin Tang · Yayun Pu · Dajun Zhai · Zhongming Cao · Jie Chen**

**Abstract** Polyhedral oligomeric silsesquioxanes (POSS) nano-particles reinforced Sn–3.0Ag–0.5Cu–xPOSS (x = 1, 3, 5) composite solders were prepared and were reflowed on Cu substrates at 543 K. Then, the solder joints were isothermal aged at 393 K for 24 and 48 h, respectively. Microstructural evolution of the solder joints were observed by scanning electron microscopy and the influence of POSS nano-particles on the solder joint were investigated. The results showed that β-Sn primary phase was refined and the number of grain boundary increased with the addition of POSS nano-particles. The growth rates of intermetallic compounds (IMCs) layer were suppressed by the adsorption affection of POSS nano-particles to the IMCs layer during isothermal aging. Moreover, the dissolution process of the IMCs layer, which was accompanied by with the growth of the IMCs layer, changed the morphology of the IMCs layer. The growth rate and the dissolution rate of the IMCs layer in Sn–3.0Ag–0.5Cu–3POSS/Cu composite solder joint were the lowest.

## 1 Introduction

The need of high-density I/O for integrated circuit designs has driven the development of flip-chip technologies in the contemporary electronic packaging industry. For flip-chip packages, the solder interconnects serviced as electrical and thermal paths as well as structural supports, which leads to serious reliability issues because the functionality of the entire package relies on the integrity of solder interconnects [1]. In order to ensure the mechanical reliability of solder joints under service conditions, a thin, continuous and uniform intermetallic compounds (IMCs) layer between solder and substrate is desirable. However, due to the inherently brittle nature of IMC layers and their tendency to generate structural defects, too thick IMC layer at the solder/substrate interface may degrade the fatigue and fracture strengths of solder joints, leading to poor reliability of electronic devices [2]. When electronic devices operate in service at high temperature, Sn/Cu IMC layer thickens at a high rate and the microstructure of solder matrix coarsens easily, which leads to a negative impact on the reliability of the solder joints [3]. So, to employ a new lead-free solder to solve these problems is necessary.

Recently, nano-composite lead-free solders by mechanically adding nano-sized particles into lead-free solder matrices have been developed in the electronic packaging materials industry to improve the creep and thermo-mechanical fatigue resistance of solder joints [4]. The particles which usually have been selected to fabricate the composite lead-free solders include (1) metal particles, such as Ag, Cu, Ni, Pt and Co. In particular, Co, Pt and Ni were very effective in suppressing the growth of IMC layers [5]; (2) multi-walled carbon nanotubes (MWCNTs) and single-wall carbon nanotubes (SWCNTs). Mechanical characterization [6, 7] results revealed that the presence of larger weight fractions of MWCNTs and SWCNTs in solder matrices led to an improvement of shear strength and microhardness of solder joints; (3) ceramic particles, such as $Zr_2O$ [8], SiC [9], $Al_2O_3$ [10] and $TiO_2$ [11], which significantly enhanced the hardness, tensile strength and creep resistance of nano-composite solders. However, particles mentioned above are generally prone to coarsening at high temperatures [4]. Facing that challenge, nano-structure polyhedral oligomeric silsesquioxanes (POSS) molecule, which was regarded as a new kind of polymeric material and

J. Shen (✉) · Q. Tang · Y. Pu · D. Zhai · Z. Cao · J. Chen
Department of Material Science and Engineering, Chongqing University, Chongqing 400044, China
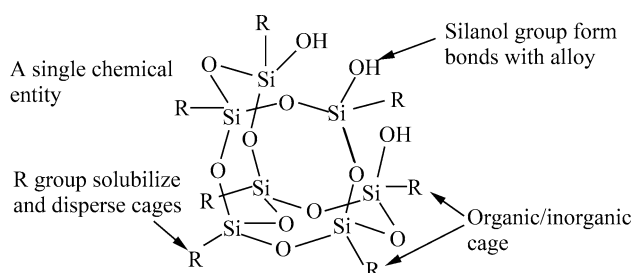e-mail: shenjun2626@163.com; shenjun@cqu.edu.cn

**Fig. 1** Anatomy of POSS molecule

would not easily coarsen, was introduced within solder alloys. Figure 1 shows the anatomy of a POSS molecule [12]. It consists of a cage-like inorganic inert core with a Si–O tetrahedral structure, seven inert R groups and organic active functional groups (–OH). Inert inorganic core makes the heat resistance and mechanical properties of composite material better. –OH groups of POSS molecules strongly bounded with metallic matrix by the formation of Si–O–Sn bonds within the grains and at grain boundaries of the solder alloy. The combination of Si–O–M (M = metal) bonding and the presence of seven inert R groups on the POSS cage prevent agglomeration of these reinforcement particles during soldering processing. In addition, POSS molecules do not dissociate from base solder alloy once it is embedded because Si–O and Si–O–M bonds are thermodynamically favorable [13, 14].

Lee and Subramanian [13] systematically investigated the effects of POSS-trisilanol and POSS-disilanol cages on the properties of eutectic Sn–Ag–POSS and Sn–4.0Ag–0.5Cu–POSS composite solder matrices. The results of this study validated the surface active, inert nano-structured chemical rigid cages pinned the grain boundary of solder alloys, which lead to an improvement of the thermo-mechanical fatigue performance between −15 and 150 °C up to 1,000 cycles. Tai et al. [15] investigated the effects of POSS nano-particles on the microstructures and microhardness of Sn–Ag solder alloy. The results indicated that due to the incorporation of the nano-structured POSS particles with surface active and high surface free energy, the microstructures of composite solders revealed finer IMCs in the solder matrix compared with eutectic Sn–3.5Ag solder. The refined $Ag_3Sn$ IMCs in Sn–3.5Ag–POSS composite solder matrix, acting as a strengthening phase in the solder matrix, enhanced the microhardness of the composite solders. However, few researches focused on the influence of POSS nano-particles on the growth of IMC layers of the solder joints during isothermal aging.

In this paper, by adding different proportion POSS nano-particles into Sn–3.0Ag–0.5Cu matrix solders (recommended by Japan JEITA) investigates the influence of POSS molecules on the microstructural evolutions of solder joints during isothermal aging.

## 2 Experimental procedure

Sn–3.0Ag–0.5Cu–xPOSS composite solders pastes (where x is the mass fraction of POSS nano-particles, x = 1, 3, 5 wt%) were prepared by mechanically stirring. POSS nano-particles, Sn–3.0Ag–0.5Cu solder powders and no-clean flux (the weight percentage of flux added was around 40–50 wt%) were mixed in a ceramic crucible for 30 min to ensure a homogeneous distribution of POSS reinforcing particles in the solder pastes. The mixed paste was screen printed on a polished alumina plate, then reflowed (BTU VIP-70 N) at the temperature of 523 K for about 1 min to prepare the composite balls. The fabricated solder balls were cooled down to room temperature in air ambient with a diameter of 1 mm.

After the preparation of the composite solders, a small amount of composite solder balls was melted on the substrate in a furnace (SX-4-10). The substrates used in this experiment were 99.99 % purity Cu plates (15 × 10 × 3 mm). They were polished with diamond powders and degreased in ethanol (with 1 vol% HCL) so as to remove surface oxides and contaminants. Then the specimens were heated to a temperature of 543 K for 3 min and then cooled down to room temperature in air ambient.

After reflowing, the specimens were thermally aged in a thermal humidity chamber (EBS-SDJ63) at 393 K for 24 and 48 h. All the cross-sections of specimens after tests were embedded in epoxy resin and prepared by standard metallographic procedures (grinding, polishing and etching with a solution of 5 vol% $HNO_3$ + 92 vol% $C_2H_5OH$ + 3 vol% HCl).

Energy dispersive X-ray spectroscopy (EDS) was employed to examine the distribution of POSS nano-particles in Sn–3.0Ag–0.5Cu–xPOSS composite solders. Scanning electron microscopy was utilized to observe the evolution of the microstructures of the solder matrices and IMC layer.

## 3 Results and discussion

### 3.1 Microstructural evolution of IMCs layer

Figure 2 shows the microstructural evolution of IMCs layer in Sn–3.0Ag–0.5Cu/Cu solder joints and Sn–3.0Ag–0.5Cu–xPOSS/Cu (x = 1, 3, 5) composite solder joints during isothermal aging at 393 K for 24 and 48 h, respectively. After reflowing for 3 min at 543 K, a homogeneous and continuous IMCs layer formed in Sn–3.0Ag–0.5Cu/Cu solder joint while a dendrite-like IMCs layer were observed in Sn–3.0Ag–0.5Cu–xPOSS/Cu composite solder joints. After isothermal aged for 48 h, all IMCs layer thickened with different growth rate. Notes

**Fig. 2** The SEM images of IMCs layer formed in four types of solder joints during isothermal aging, **a** Sn–3.0Ag–0.5Cu/Cu solder joint, 0 h, **b** Sn–3.0Ag–0.5Cu/Cu solder joint, 24 h, **c** Sn–3.0Ag–0.5Cu/Cu solder joint, 48 h, **d** Sn–3.0Ag–0.5Cu–1POSS/Cu composite solder joint, 0 h, **e** Sn–3.0Ag–0.5Cu–1POSS/Cu composite solder joint, 24 h, **f** Sn–3.0Ag–0.5Cu–1POSS/Cu composite solder joint, 48 h, **g** Sn–3.0Ag–0.5Cu–3POSS/Cu composite solder joint, 0 h, **h** Sn–3.0Ag–0.5Cu–3POSS/Cu composite solder joint, 24 h, **i** Sn–3.0Ag–0.5Cu–3POSS/Cu composite solder joint, 48 h, **j** Sn–3.0Ag–0.5Cu–5POSS/Cu composite solder joint, 0 h, **k** Sn–3.0Ag–0.5Cu–xPOSS/Cu composite solder joint, 24 h and **l** Sn–3.0Ag–0.5Cu–xPOSS/Cu composite solder joint, 48 h
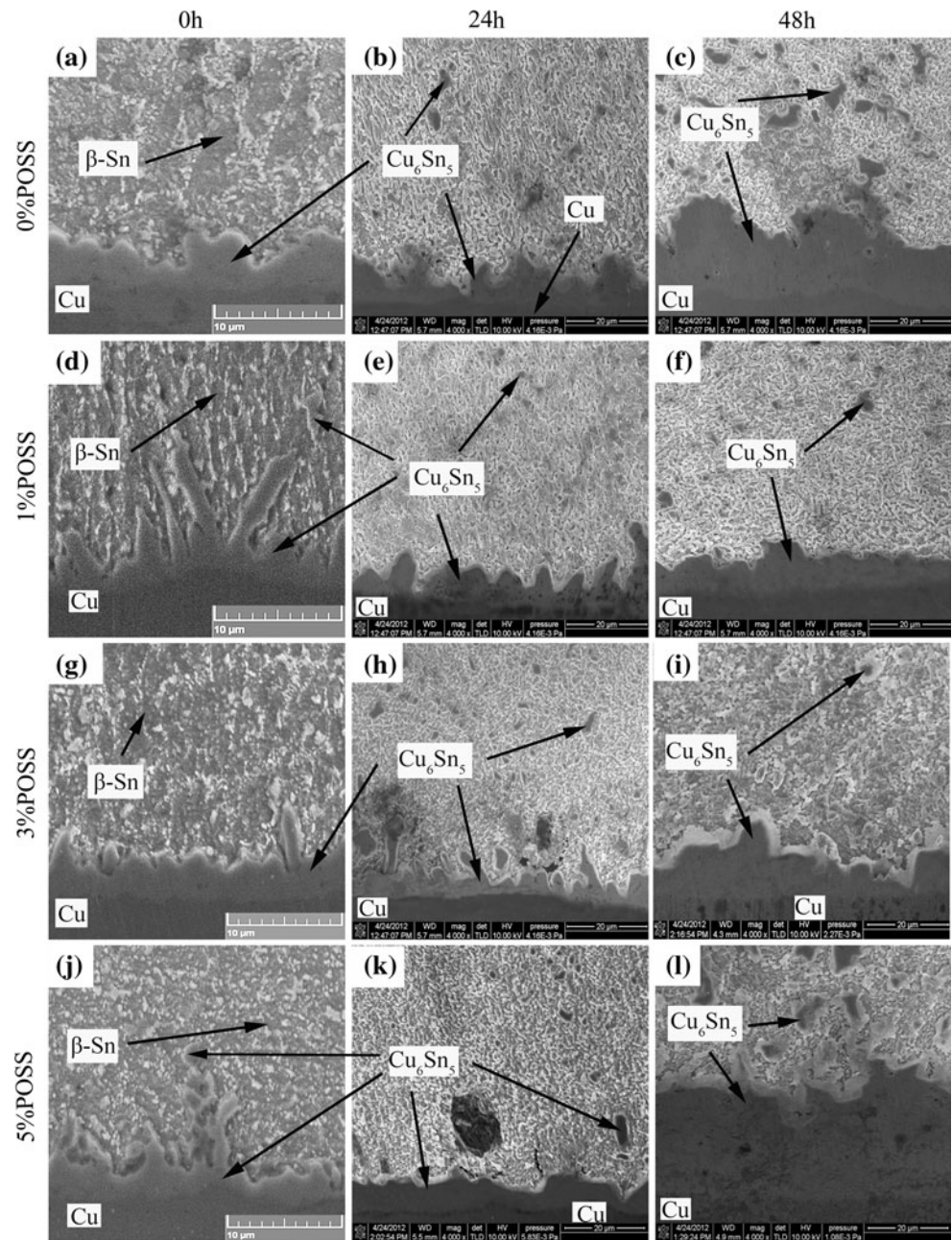


only in Sn–3.0Ag–0.5Cu–3POSS/Cu composite solder joint, a thin and uniform scallop-type IMCs layer formed obviously.

### 3.2 The evolution of the average thickness of IMCs layer during isothermal aging

The average thickness of IMCs layer in Sn–3.0Ag–0.5Cu/Cu solder joint and Sn–3.0Ag–0.5Cu–xPOSS/Cu composite solder joints (x = 1, 3, 5) against isothermal aging time are shown in Fig. 3. It can be seen that the growth rates of $Cu_6Sn_5$ IMCs layer in the four solder joints were different.

The reaction at the substrate/solder interface involves the net effects of numerous growth dynamics factors in some coordinated fashion, such as volume diffusion, grain boundary diffusion, grain boundary grooving and grain coarsening [16]. Nano-structured POSS nano-particles added into eutectic Sn–3.0Ag–0.5Cu lead free solders are mainly consisted of O and Si elements. So the distribution of O and Si elements can represent the distribution of POSS nano-particles. Figure 4 shows O and Si elements are well-dispersed and are present in higher concentration along the grain boundary in Sn–3.0Ag–0.5Cu–3POSS composite solders, which indicates POSS-particles mainly
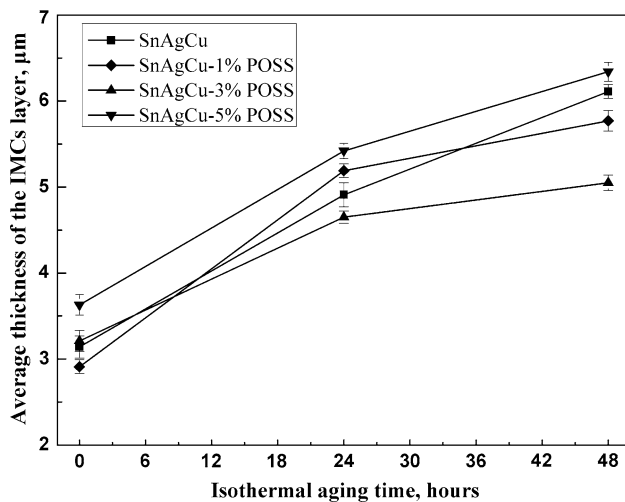
**Fig. 3** The relationship between the dissolving rate of the IMC layers formed in the solder joints and the isothermal aging time

distributed in the grain boundary in Sn–3.0Ag–0.5Cu–3POSS composite solders. Actually, EDS results of Sn–3.0Ag–0.5Cu–1POSS and Sn–3.0Ag–0.5Cu–5POSS composite solders give the same phenomenon. On the one hand, POSS nano-particles did not melt in soldering process as its high melt point. The melted solder alloy nucleated and grew up by attaching on the surface of the additional particles, leading the increase of grain boundary and the decrease of the average grain size of β-Sn (see Fig. 2a, d, g, j) and $Ag_3Sn$ [15]. The presence of grain boundary accelerates the growth rate of the IMC layers demonstrated by Bader et al. [17]. And on the other hand, part of the inert nano-particles adsorbed at the interface of IMCs layer by forming Si–O–Sn bond (Fig. 5). The adsorption to the IMCs layer decreased the surface energy and hampered the excessive growth of the IMCs layer. During isothermal aging between 0 and 24 h, the growth rate of the IMCs layer at the solder joints was seen as: $r_{Sn–3.0SAg–0.5Cu–3POSS/Cu} < r_{Sn–3.0SAg–0.5Cu–5POSS/Cu} < r_{Sn–3.0SAg–0.5Cu/Cu} < r_{Sn–3.0SAg–0.5Cu–1POSS/Cu}$ ($r$ is the growth rate of the IMCs layer). It shows that the growth rates of the

IMCs layer in Sn–3.0Ag–0.5Cu–1POSS/Cu composite solder joint was higher than that in Sn–3.0Ag–0.5Cu/Cu solder joint. That is because β-Sn was refined and the number of grain boundary increased in Sn–3.0Ag–0.5Cu–1POSS composite solder matrix, which accelerated the growth of the IMCs layer. The adsorption of the POSS nano-particles to the IMCs layer was relatively weak. Figure 5b shows the amounts of the POSS nano-particles in Sn–3.0Ag–0.5Cu–1POSS/Cu composite solder joint was fewer than that in other composite solder joints (see Fig. 5c, d). With an increase of the addition of POSS nano-particles, the adsorption effect of POSS nano-particles to the IMCs layer was enhanced. So the thickness of the IMCs layer in Sn–3.0Ag–0.5Cu–3POSS/Cu composite solder joint was the smallest. Even though the adsorption effect of POSS nano-particles in Sn–3.0Ag–0.5Cu–5POSS/Cu composite solder joint was the strongest (Fig. 5d shows the additional POSS nano-particles aggregated together and closed the $Cu_6Sn_5$ reaction interface), the thickness of the IMCs layer in this joint was higher than that in Sn–3.0Ag–0.5Cu–3POSS/Cu composite solder joint as there was a refiner grain size when the amount of POSS nano-particles added is higher to 5 wt%.

After isothermal aged 48 h, the growth rate of the IMCs layer at the solder joints was changed to $r_{Sn–3.0SAg–0.5Cu–3POSS/Cu} < r_{Sn–3.0SAg–0.5Cu–1POSS/Cu} < r_{Sn–3.0SAg–0.5Cu–5POSS/Cu} < r_{Sn–3.0SAg–0.5Cu/Cu}$. During isothermal aging between 24 and 48 h, the growth of the IMC layers at Sn–3.0Ag–0.5Cu/Cu solder was affected by grain coarsening, which led the thickness increased quickly. But as the pinning effect of POSS nano-particles to the grain boundary, the grains in the composite solders did not coarsen easily. So the thickness of the IMCs layer in Sn–3.0Ag–0.5Cu/Cu solder joints reached the highest value after isothermal aged 48 h. Besides that, $Cu_6Sn_5$ gradually translated from metastable into steady state with the extension of the aging time. The interface energy and surface energy of $Cu_6Sn_5$ further reduced [2]. So the slopes of $Cu_6Sn_5$ thicknesses in the three composite solder joints between isothermal aged 24 and 48 h were smaller compared to that between isothermal aged 0 and 24 h.
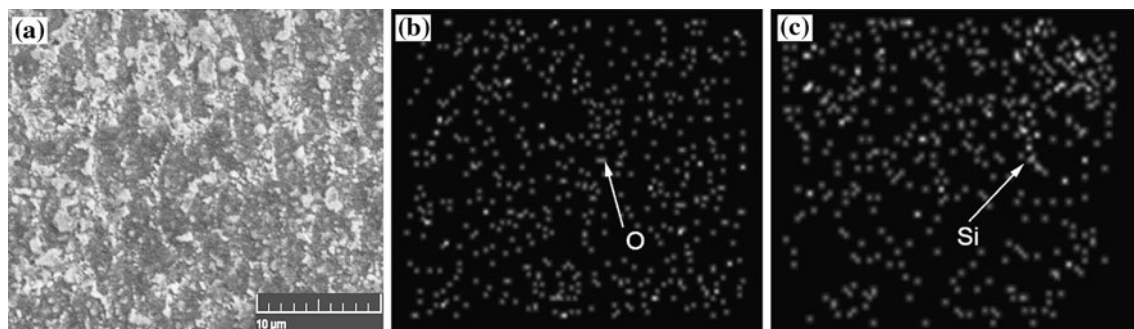


**Fig. 4** The distribution of Si and O elements in Sn–3.0Ag–0.5Cu–3POSS composite solder matrix
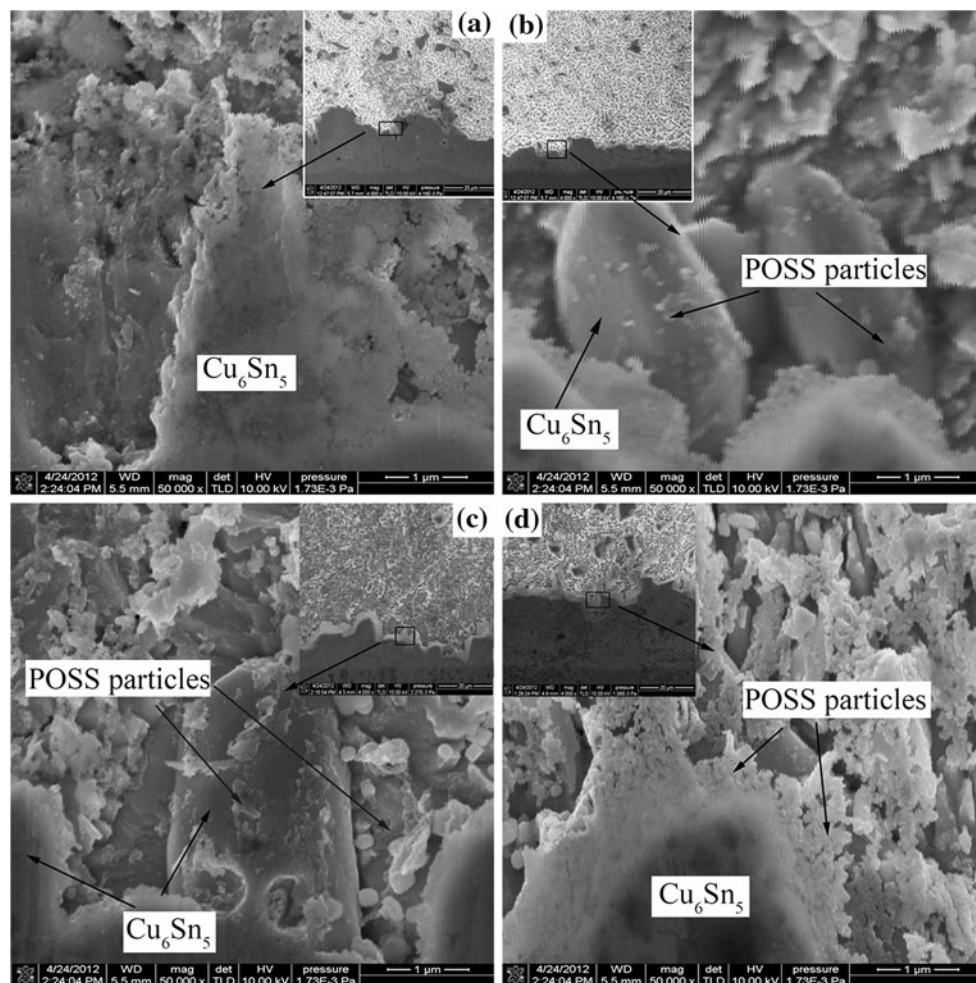
**Fig. 5** High magnification SEM images showing the morphologies of POSS nano-particles at the Sn–3.0Ag–0.5Cu–xPOSS/Cu composite solder joints after isothermal aged for 48 h, **a** Sn–3.0Ag–0.5Cu/Cu solder joint, **b** Sn–3.0Ag–0.5Cu–1POSS/Cu composite solder joint, **c** Sn–3.0Ag–0.5Cu–3POSS/Cu composite solder joint and **d** Sn–3.0Ag–0.5Cu–5POSS/Cu composite solder joint

### 3.3 The dissolution rate of IMCs layer

Obviously, with the additions of POSS nano-particles, not only the thicknesses of the IMCs layer in the solder joint were different, but also the morphologies of the IMCs layer were changed. It should be stressed that numbers of irregular block $Cu_6Sn_5$ displayed in Sn–3.0Ag–0.5Cu solder matrix and Sn–3.0Ag–0.5Cu–xPOSS composite solder matrices during the whole process (see Fig. 2). This is because both during reflowing process and isothermal aging, few of the solid $Cu_6Sn5$ IMCs layer dissolved into the solder matrices. However, the dissolving mechanism and the dissolving effects of $Cu_6Sn_5$ on the morphology and the thickness of the IMCs layer are different between reflowing process and isothermal aging process.

Dybkov's research manifested that regarding the kinetics of dissolution of a solid in a liquid by a solid/liquid interfacial reaction, the rate of dissolution of the IMCs layer in a molten solder during reflowing may be expressed by the equation [18]:

$$\frac{dc}{dt} = k \times \frac{s}{v}(c_s - c) \tag{1}$$

where $\frac{dc}{dt}$ is the rate of dissolution of the $Cu_6Sn_5$ layer, $k$ is the dissolution rate constant of $Cu_6Sn_5$, $s$ is the interfacial area of the $Cu_6Sn_5$ layer in contact with the molten solders, $v$ is the volume of the molten solder, $c_s$ is the saturation concentration of Cu in the molten solder at the reflowing temperature, and $c$ is the concentration of Cu in the molten solder measured at time $t$. In this test, the rate of dissolution of the $Cu_6Sn_5$ layer, $\frac{dc}{dt}$, could not be calculated quantitatively as $k$ was not given. Otherwise, the microstructural observations showed us no $Cu_6Sn_5$ was formed in Sn–3.0Ag–0.5Cu solder matrices (see Fig. 2a) while small amounts of $Cu_6Sn_5$ was formed in Sn–3.0Ag–0.5Cu–xPOSS composite solder matrices (see Fig. 2d, g, j). It was

worth noting that a serrated-like irregular IMCs layer formed in Sn–3.0Ag–0.5Cu–xPOSS/Cu composite solder joints (see Fig. 2d, g, j). Hence there was a relationship between the dissolution of the solid $Cu_6Sn_5$ and the morphologies of the IMCs layer. According to the above Eq. (1), due to $v$ is slight and $k$, $c_s - c$ is almost constant during reflowing [19], the rate of dissolution of the $Cu_6Sn_5$ layer into the molten solder is almost controlled by the interfacial area of the IMCs layer in contact with the molten solder $s$. In Sn–3.0Ag–0.5Cu–xPOSS/Cu composite solder joints during reflowing, POSS nano-particles did not react with $Cu_6Sn_5$ IMCs layer and accumulated inhomogeneously at the reaction interface, which impede the molten solder from contacting with the $Cu_6Sn_5$ IMCs layer in part and reduce the interfacial area, $s$. So, in some areas of the surface of $Cu_6Sn_5$ IMCs layer, the rate of growth of the IMCs layer was slower than in other areas, and therefore, this led to the serrated-like of the $Cu_6Sn_5$ IMCs layer in Sn–3.0Ag–0.5Cu–xPOSS/Cu composite solder joint.

After isothermal aged for 24 h, a number of $Cu_6Sn_5$ formed in the four solder matrices, and it became more and more after isothermal aged for 48 h (see Fig. 2b, c, e, f, h, i, k, l). The researches of Tu et al. [20] and Tu [21] indicated scallop-type grains (or hemispherical grain) are stable when in contact with molten solder, but the layer-type grains (or cylindrical grain) are stable when in contact with solid solder. So, during isothermal aging, scallop-type $Cu_6Sn_5$ was morphologically unstable and translated to layer-type $Cu_6Sn_5$ with the minimization of interfacial and grain boundary energies. With the transformation from hemispherical grain into cylindrical grain, the grain channels of $Cu_6Sn_5$ will disappear and Cu elements can not reach the interfacial of IMCs layer and solders. Interfacial reaction stopped also. Then the ripening reaction occurred among part of the scollop $Cu_6Sn_5$. Without the changes of grain volume, hemispherical $Cu_6Sn_5$ transformed into spheroids by deceasing surface, and departed from main IMCs layer and moved towards the solid solder matrix through grain boundary diffusion and volume diffusion. The rates of the dissolution of $Cu_6Sn_5$ were different by comparing the amount of $Cu_6Sn_5$ in the four solder matrices (see Fig. 2c, f, i, l). It shows the dissolution rates of the IMCs layer in Sn–3.0Ag–0.5Cu–xPOSS/Cu composite solder joints were lower than that in Sn–3.0Ag–0.5Cu/Cu solder joint and it reached the smallest value in Sn–3.0Ag–0.5Cu–3POSS/Cu composite solder joint. This is because part of the additional POSS nano-particles decreased the interfacial energy of $Cu_6Sn_5$ layer by accumulating at the reaction interface, which effectively reduced the driving force of transformation from hemispherical $Cu_6Sn_5$ into cylindrical $Cu_6Sn_5$, leading the reducing of the dissolution rate of the IMCs layer in Sn–3.0Ag–0.5Cu–xPOSS/Cu solder joints.

## 4 Conclusions

In this study, microstructural evolutions of Sn–3.0Ag–0.5Cu–xPOSS/Cu solder joint and Sn–3.0Ag–0.5Cu–xPOSS/Cu (x = 1, 3, and 5) composite solder joints during isothermal aging were investigated. The conclusions may be summarized as follows:

1. With the addition of POSS nano-particles into Sn–3.0Ag–0.5Cu solder matrix, β-Sn phase was refined and the number of grain boundary was increased. Moreover, part of POSS nano-particles adsorbed on the IMCs layer in Sn–3.0Ag–0.5Cu–xPOSS/Cu solder joints, leading the morphologies and the growth rates of the IMCs layer changed. In particular, the growth rate of the IMCs layer in Sn–3.0Ag–0.5Cu–3POSS/Cu solder joint was the lowest.

2. During reflowing and isothermal aging, the growth process of the IMCs layer was accompanied by with the dissolution of the IMCs layer. The additional POSS nano-particles accumulating at the IMCs layer surface not only impeded solid $Cu_6Sn_5$ dissolving into the molten solder but also reduced the interfacial energy of IMCs layer in Sn–3.0Ag–0.5Cu–xPOSS/Cu composite solder joints. The dissolving rate reached the smallest value in Sn–3.0Ag–0.5Cu–3POSS/Cu composite solder joint by comparing.

## References

1. Y.S. Lai, C.L. Kao, Microelectron. Reliab. **46**, 915 (2006)
2. T. Laurila, V. Vuorinen, J.K. Kivilahti, J. Mater. Sci. Eng. R **49**, 1 (2005)
3. J. Shen, Y.C. Chan, S.Y. Liu, Acta Mater. **57**, 5196 (2009)
4. J. Shen, Y.C. Chan, Microelectron. Reliab. **49**, 223 (2009)
5. M. Amagai, Microelectron. Reliab. **48**, 1 (2008)
6. S.M.L. Nai, J. Wei, M. Gupta, J. Alloy. Compd. **473**, 100 (2009)
7. K.M. Kumar, V. Kripesh, A.A.O. Tay, J. Alloy. Compd. **450**, 229 (2008)
8. J. Shen, Y.C. Chan, Y.J. Han, Y.M. Tian, H.X. Gao, Mater. Sci. Eng. A **441**, 135 (2006)
9. P. Liu, P. Yao, J. Liu, J. Electron. Mater. **37**, 874 (2008)
10. X.L. Zhong, M. Gupta, J. Phys. D Appl. Phys. (2008). doi:10.1088/0022-3727/41/9/095403
11. D.C. Lin, G.X. Wang, T.S. Srivatsan, M. Al-Hajri, M. Petraroli, Mater. Lett. **57**, 3193 (2002)
12. S.H. Phillips, T.S. Haddad, S.J. Tomczak, Curr. Opin. Solid State Mater. Sci. **8**, 21 (2004)
13. A. Lee, K.N. Subramanian, J. Electron. Mater. **34**, 1399 (2005)
14. R. Zhang, G.C. Xu, X.T. Wang, F. Guo, A. Lee, K.N. Subramanian, J. Electron. Mater. **39**, 2513 (2010)

15. F. Tai, F. Guo, Z.D. Xia, Y.P. Lei, Y.W. Shi, J. Mater. Sci.: Mater. Electron. **21**, 702 (2010)
16. M. Schaefer, R.A. Fournelle, J. Liang, J. Electron. Mater. **27**, 1167 (1998)
17. S. Bader, W. Gust, H. Hieber, Acta Metall. Mater. **43**, 329 (1995)
18. V.I. Dybkov, *Growth Kinetics of Chemical Compound Layers* (Cambridge International Science, Cambridge, 1998)
19. H.K. Kim, K.N. Tu, Phys. Rev. B **53**, 16027 (1996)
20. K.N. Tu, A.M. Gusak, M. Li, J. Appl. Phys. **93**, 1335 (2003)
21. K.N. Tu, *Solder Joint Technology* (Springer, New York, 2007), pp. 127–151